

# Turning Low-Cost Filter Papers to Highly Efficient Membranes for Oil/Water Separation by Atomic-Layer-Deposition-Enabled Hydrophobization

Liang Kong, Qianqian Wang, Sen Xiong, and Yong Wang\*

State Key Laboratory of Materials-Oriented Chemical Engineering, College of Chemistry and Chemical Engineering, Nanjing Tech University, 5 Xin Mofan Street, Nanjing, China, 210009

**ABSTRACT:** It remains a great challenge for the simple and affordable production of membranes for oil/water separation. We prepare low-cost but highly efficient paper-based membranes for oil/water separation through hydrophobic modification to filter papers. The simple modification contains only two steps: a thin layer of aluminum oxide is first coated on the surface of the filter paper by atomic layer deposition, and silane molecules are subsequently coupled on the precoated aluminum oxide layer via their reaction with hydroxyl groups on the surface. Both the alumina layer and the silanization layer are very thin with a total thickness less than 10 nm. The modified filter paper is endowed with strong hydrophobicity and oleophilicity, therefore exhibits strongly retarded permeation to water and enhanced permeation to nonpolar oils. The modified filter paper is demonstrated to show excellent separation efficiencies greater than 90% in the separation of various types of oils and organic solvents from their mixtures with water. The paper-based membranes prepared in this work are distinguished among others for their low-cost substrates and simple modification route. This modification method is expected to be easily extended to hydrophobize a diversity of other substrates.

## 1. INTRODUCTION

Frequent oil spill accidents may lead to severe environmental pollution, as well as massive financial and energy loss.<sup>1,2</sup> Oily wastewater emitted from petrochemical and steel industries has also become the major pollutant worldwide.<sup>3,4</sup> Conventional separation methods, such as gravity separation and combustion, have the drawbacks of low efficiency and generation of secondary pollutants, which hinder their large-scale application.<sup>3</sup> Selective absorption of oily liquids from water using oleophilic and/or hydrophobic porous materials could be considered as an efficient and inexpensive approach. For instance, carbon and polyurethane (PU) foams have been used as effective absorbent substrates; however, the absorption is a discontinuous separation process, as the absorbents will be saturated after uptaking a certain amount of oils. The oil absorbents require regeneration before they can be reused, and in many cases, the absorbents cannot be regenerated at all or can only be recycled for very limited times.<sup>5,6</sup>

Membrane filtration, which can be operated in the continuous mode, has been vastly developed in the oil/water separation system due to its energy-saving and cost-efficient features.<sup>7</sup> A number of porous materials have been used as substrates for oil/water separation after appropriate surface modifications, and commonly used substrates include metal meshes, synthetic fabrics, cottons, porous carbon, polymeric membranes prepared by the phase inversion method, etc.<sup>5,8–13</sup> Some of the substrates, such as porous carbon, are strongly oleophilic and hydrophobic as their intrinsic nature; thus, they can be directly used for oil/water separation to allow the penetration of oil, meanwhile retaining water. For other substrates, for example, polyester or cotton fabrics, which are rather hydrophilic or insufficiently hydrophobic, additional hydrophobization is essential to modify the surface of the

substrate only wettable to oils.<sup>11</sup> To this end, a variety of strategies, including chemical grafting or physical deposition of strongly hydrophobic molecules onto the substrate surface, have been successful in turning originally hydrophilic surfaces into highly hydrophobic and oleophilic ones.<sup>4</sup> Many of the above-mentioned membranes have demonstrated excellent performances in the separation of oil/water mixtures; however, it is still highly demanding for high-performance membranes prepared from easily available substrate materials through simple and affordable modification methods.

Herein, we report on highly efficient membranes based on low-cost filter papers subjected to simple hydrophobic modification. Filter papers are widely used as porous materials to separate solids from liquids.<sup>14</sup> The main composition of filter papers is cotton fibers, which show strong hydrophilicity. The coating of hydrophobic materials onto hydrophilic filter papers would obtain surface-modified filter papers with the capability for oil/water separation. Filter papers with the pore size of 20–25  $\mu\text{m}$  were used as substrates and first coated with a layer of  $\text{Al}_2\text{O}_3$  by atomic layer deposition. It has been reported that the deposition of oxide layers could endow the substrates with hydrophilicity, which means the  $\text{Al}_2\text{O}_3$ -deposited surface contains more hydroxyl groups.<sup>7</sup> After the coupling with silane, the filter papers will have hydrophobicity and then could be used as a membrane for the effective separation of oil/water mixtures.

**Received:** July 18, 2014

**Revised:** September 22, 2014

**Accepted:** September 30, 2014

**Published:** September 30, 2014

## 2. EXPERIMENTAL DETAILS

**2.1. Materials.** The filter paper sheets with maximum pore diameter of 20–25  $\mu\text{m}$  and ash content less than 0.15% were purchased from Hangzhou Specialized Paper Co., Ltd., and were used as substrates for ALD of  $\text{Al}_2\text{O}_3$ . Trimethylaluminum (TMA, 99.99%, Nanjing University) and deionized water (conductivity: 8–20  $\mu\text{s}/\text{cm}$ , Wahaha Co.) were used in the ALD process as the metal precursor and oxidant source, respectively. 3-Methacryloxypropyltrimethoxysilane (KH-570, 98%) purchased from Meryer (Shanghai) Chemical Technology Co., Ltd., was used as the silane coupling agent. Diesel oil was obtained from local suppliers, and organic solvents including chloroform, cyclohexane, and ethanol of AR grade were commercially acquired and used without further treatment. Phenolphthalein and Solvent Blue 35 obtained from local suppliers were used to indicate water and oil by coloring them red and blue, respectively. A liquid filtration cell (FB-04T, Auto Science) was used to separate oil/water mixtures.

**2.2. Atomic layer deposition on filter papers.** The filter papers were coated by  $\text{Al}_2\text{O}_3$  using a commercialized ALD reactor (Savannah S100, Cambridge NanoTech). The reactions were performed at the temperature of 80  $^\circ\text{C}$  under vacuum (0.7 Torr), where the chamber was preheated to the deposition temperature for at least 30 min. Nitrogen with ultrahigh purity (99.99%) was used as precursor carrier gas at a mass flow rate of 20 sccm. In a typical ALD cycle, TMA and deionized water were alternatively pulsed into the reactor for 0.015 s with the exposure time of 10 s, and the chamber was immediately purged with nitrogen for 30 s to sweep off the excessive precursors. The applied numbers of cycles for ALD of  $\text{Al}_2\text{O}_3$  were 10, 30, 60, 90, 150, and 200, respectively.

**2.3. Silane coupling of the deposited filter papers.** KH-570 was dissolved in ethanol to produce silane coupling solution at the concentration of 5 wt %. The  $\text{Al}_2\text{O}_3$ -deposited filter papers were cut into circular pieces with the diameter of 25 mm and immersed in the coupling solution under moderate magnetic stirring for 4 h at room temperature. The resulting filter paper pieces were washed with ethanol for three times and dried at 70  $^\circ\text{C}$  for 3 h.

**2.4. Characterizations.** The surface morphology of the filter papers was performed on a Hitachi S-4800 field emission scanning electron microscope (FESEM) operated at 5 kV. The filter papers were sputtering-coated with a thin layer of Au/Pd alloy to avoid surface charging of the samples during SEM observations. Surface elemental analysis of the filter paper was operated at 20 kV and 10 mA using an Oxford INCA 350 energy dispersive X-ray microanalysis system (EDX) attached to the SEM instrument. The water contact angles were measured on a MAIST Vision Dropmeter A-100 contact angle goniometer. For each sample, at least five different sites were tested, and the mean value was recorded. X-ray photoemission spectroscopy (XPS) measurements were recorded on a Kratos AXIS Ultra DLD XPS spectrometer. X-rays of energy  $h\nu = 1486.6$  eV used a monochromatic rotating anode Al  $K\alpha$  source and a charge neutralizer. The ejected photoelectrons were analyzed by an electron energy analyzer at a pass energy of 30 eV. The effective instrumental step size is 0.05 eV.

**2.5. Evaluation of the affinity performances.** Solvent blue 35 was added into diesel oil while phenolphthalein was added into water at the pH of 11.5 to identify each liquid. Basically the pristine and modified filter papers were placed on

top of the vial, and then water (red) and diesel oil (blue) were added continuously using a pipet to observe the affinity of modified filter paper to water and oil.

**2.6. Evaluation of the permeability and separation performances.** A filtration cell (FB-04T, Auto Science) was used to measure the permeability and separation performance of the modified filter paper at room temperature. The filtration cell contains two pieces of glass tubes, and the modified filter paper is clamped in between. Only oils and organic solutions were dyed blue to distinguish from the mixture of colorless water and colored oils. For the pristine filter papers with pore size of tens of microns, liquid could penetrate the filter paper driven by gravity.

For the permeability test, filter paper before and after modification was positioned in the filtration cell and 30 mL of liquid (water, diesel oil, chloroform, and cyclohexane, respectively) was added to measure the amount of liquid penetrated through the filter paper within 1 min. The pristine filter paper was tested as reference. Each sample was measured six times, and the mean value was reported as the permeability of the filter paper.

The filtration cell was then used to test the separation efficiency of the oil/water mixture. A mixture containing water and oils such as diesel oil, chloroform, and cyclohexane was added into the cell, respectively. Taking diesel oil as an example, water and diesel oil were added simultaneously into the upper tube and diesel oil would float on top of the water due to its relatively smaller density. The two components were mixed scrupulously via nitrogen bubbling at a certain flow rate which ensures the sufficient contact of diesel oil to the surface of the filter paper, and diesel oil was permeated through the filter paper immediately after the commencing of bubbling. The color of the mixture in the upper tube became lighter with the ongoing separation process. Diesel oil was filtered and collected, and the separation process was terminated as soon as the colored oils were filtered completely from the filtration cell. The colorless water left in the filtration cell weighed as  $m_1$ , while the total amount of water added in the filtration cell weighed as  $m_0$ . The separation efficiency  $S$  (%) was calculated as  $S = m_1/m_0$ . Water and organic solvents were mixed with different mass ratios of 1:1, 5:1, and 10:1 to test the separation efficiency of the modified filter paper.

## 3. RESULTS AND DISCUSSIONS

**3.1. The hydrophobization process of filter papers.** It is known that the absorption/separation capacity of oil for porous hydrophobic materials was predominantly determined by the porosity, pore size, and surface morphology. From the practical perspective, the ideal porous materials should be cost-efficient, easily obtained, and recyclable.<sup>15</sup> Therefore, inexpensive filter papers with high porosity were used as substrates. However, the as-purchased filter papers have a certain affinity for both water and oil with no selectivity.

The modification method we utilized here takes only two steps,  $\text{Al}_2\text{O}_3$  deposition by ALD and silanization, both of which were based on the surface reaction to acquire ultrathin layers (Figure 1). Silane coupling agents have the advantages of great variety and low cost. However, they could only react with the hydroxyl groups via a bridging effect and combine with the substrates through the covalent bond to generate a hydrophobic monomolecular layer.<sup>16</sup> A transition layer of hydroxyl groups must be built on the surface of the filter paper before silanization to obtain the hydrophobicity. The oxide layer can

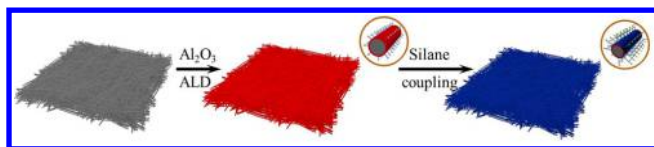


**Figure 1.** Hydrophobization process of filter papers including atomic layer deposition of  $\text{Al}_2\text{O}_3$  and silane coupling.

be coated on the surface of filter paper to acquire hydroxyl groups, and ALD has been proved to deposit an oxide layer on any possible substrate with the thickness at the angstrom level.<sup>17</sup> ALD technically works in a cyclic mode which produces material that is only one atomic layer thick for each cycle. Therefore, the thickness of the deposited layer could be precisely controlled by increasing the ALD cycle numbers.<sup>18,19</sup> In this work, the ALD technique will be exploited to deposit an  $\text{Al}_2\text{O}_3$  thin layer on the surface of the filter paper. After coupling the hydroxyl groups on the  $\text{Al}_2\text{O}_3$  layer with the silane coupling agent KH-570, hydrophobized filter papers with strong oleophilicity were achieved.

**3.2. Confirmation of the  $\text{Al}_2\text{O}_3$  deposition and silanization on filter papers.** X-ray photoelectron spectroscopy (XPS) is a significant technique due to its sensitivity to surface composition. The filter paper with 90 cycles of  $\text{Al}_2\text{O}_3$  ALD was analyzed by XPS, and the pristine filter paper was used as reference. A new characteristic peak attributed to Al  $2p$  is discernible in the XPS spectra of the deposited sample (Figure 2a, b), which indicates  $\text{Al}_2\text{O}_3$  has effectively been deposited on the surface of filter papers. It has also been noticed that the intensity of the characteristic peaks is relatively

weak, which suggests the  $\text{Al}_2\text{O}_3$  layer deposited on the filter paper is very thin. Moreover, two peaks assigned to Al  $2p$  and Si  $2p$  could be observed in Figure 2c and d of the filter paper. They could subsequently be subjected to  $\text{Al}_2\text{O}_3$  deposition and silanization, which further confirms the successful incorporation of  $\text{Al}_2\text{O}_3$  and KH-570 on the filter papers.

To further confirm the surface elemental composition, the filter paper with ALD deposition of  $\text{Al}_2\text{O}_3$  for 90 cycles was analyzed by energy dispersive X-ray spectroscopy (Figure 3a).

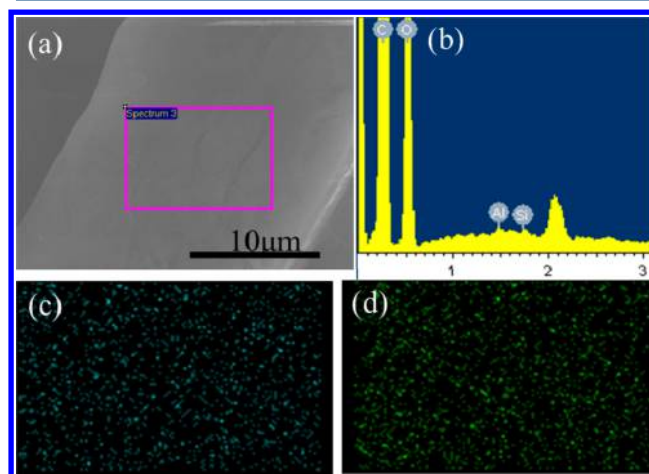


**Figure 3.** EDS analysis of the modified filter paper with 90 ALD cycles and silanization: (a) the selected area; (b) surface scanning spectrum; (c) surface distribution of Si; and (d) surface distribution of Al in the scanned area marked in (a).

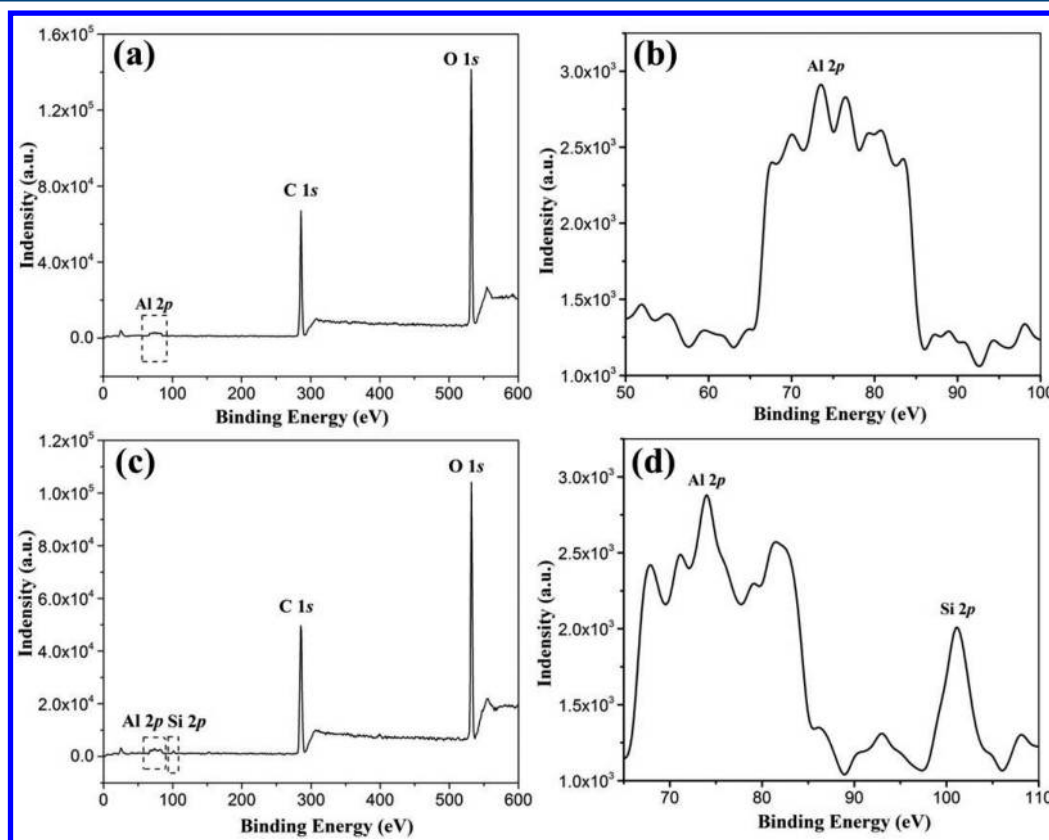


**Figure 2.** XPS spectra of the  $\text{Al}_2\text{O}_3$ -deposited filter paper (a: survey and b: Al  $2p$ ) and the silanized filter paper after  $\text{Al}_2\text{O}_3$  deposition (c: survey and d: Al  $2p$  and Si  $2p$ ).

The EDS spectrum (Figure 3b) displays new peaks of Al and Si, which indicates once again the successful deposition of  $\text{Al}_2\text{O}_3$  and the combination of silane on the surface of the filter papers. Only trace amount of Al and Si elements could be detected due to the ultrathin nature of the deposition and the silanization layer. Moreover, the signals of the Al and Si elements cannot be identified by EDS when the ALD cycle number is less than 90, which should be attributed to the extremely low concentration of Al and Si on the surface of filter papers, even lower than the instrumental detection limit.

It has been reported that there is a subsurface nucleation for ALD of oxides on polymeric substrates which typically takes place in the initial 50 cycles in the case of deposition of  $\text{Al}_2\text{O}_3$ .<sup>20</sup> In this subsurface nucleation process, the precursors penetrate into the near-surface regions of the substrate and  $\text{Al}_2\text{O}_3$  will form in the free volumes of the polymers.<sup>20</sup> Afterward, continuing ALD cycles will produce an  $\text{Al}_2\text{O}_3$  layer on the surface of the substrate at a growth rate of approximately 0.15–0.2 nm per cycle.<sup>21,22</sup> Therefore, it can roughly be estimated that the theoretical thickness of the  $\text{Al}_2\text{O}_3$  layer on the surface of the filter paper subjected to 90 ALD cycles is around 6–8 nm after the subtraction of the initial 50 cycles. Based on the covalent bond formed between the silane coupling agent and the hydroxyl-terminated substrate surface, a monomolecular layer of silane will be coupled onto the surface of  $\text{Al}_2\text{O}_3$ . As the chain length of KH-570 is around 0.99 nm,<sup>23</sup> it can consequently be calculated that the total thickness of the modification layer is less than 10 nm. Scanning of the Al and Si element distribution on the surface of the filter paper was also conducted, and it could be observed from Figure 3c and d that both elements were highly dispersed, which confirms the  $\text{Al}_2\text{O}_3$  and silane are homogeneously distributed on the surface.

**3.3. Morphology of  $\text{Al}_2\text{O}_3$ -deposited and -silanized filter papers.** SEM images were also taken to investigate the morphology of the filter papers after ALD deposition and silanization. It can be seen from Figure 4a that the filter paper

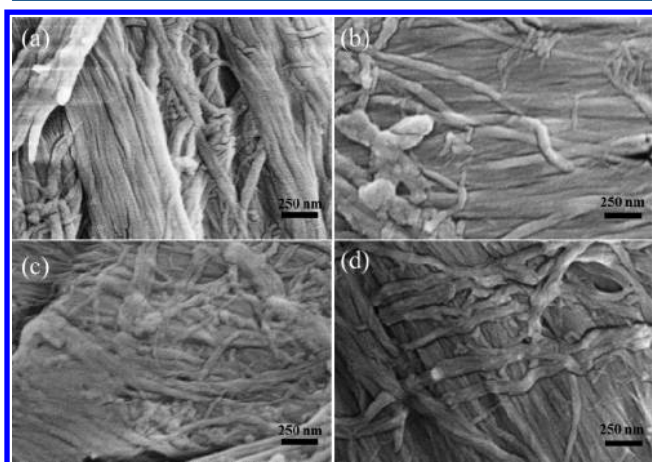


**Figure 4.** Surface SEM images of filter paper before (a) and after  $\text{Al}_2\text{O}_3$  deposition with 90 (b) and 200 (c) ALD cycles and silanization after 90 ALD cycles (d).

consists of bundles of continuous fine fibers with diameters down to a few nanometers, and gaps among the bundles serve as pores for the filtration of liquids.<sup>24</sup> After ALD deposition for 90 cycles, the large bundles are still clearly present; however, the constituent fine fibers are not easily detectable, as the deposited  $\text{Al}_2\text{O}_3$  layer might fill the in-between voids of the

fibers (Figure 4b). Further increase of the ALD cycle numbers to 200 continues to seal some small gaps between the fibers and even merge the adjacent bundles to form a continuous film in some local areas (Figure 4c). The filter paper with ALD deposition and silane coupling was also investigated, and no obvious difference could be observed compared with Figure 4b. The filter papers possessed a uniform and conformal morphology within the deposition cycles ranging from 0 to 200. No significant changes were observed from the macroscopic appearance or structure of the filter papers after a deposition number up to 200; this result is in agreement with literature reports,<sup>25,26</sup> which could be assigned to the ultrathin and conformal nature of both the deposition and the silanization layer.

**3.4. Hydrophobicity of the modified filter papers.** The analyses above have confirmed the deposition of  $\text{Al}_2\text{O}_3$  and silane coupling on the surface of filter papers. The separation capacity is an important factor to evaluate the performance of the membrane. The pristine filter paper exhibits a moderate hydrophilicity, attributed to its cellulose-based chemical nature, and it shows affinity to both water and oil. Figure 7a illustrates the wetting behavior of water and diesel oil on the surface of the pristine filter paper. Both water and oil droplets were absorbed instantly and then spread away due to the moderate hydrophilicity and large pore sizes of the filter paper. However, the spread speed of the oil droplet was slightly slower than that of the water droplet, implying the filter paper shows stronger affinity for water. It is clear that the pristine filter paper does not have selectivity between water and oil. The water contact angles on pristine filter paper and modified filter papers were measured, and bare filter paper was highly hydrophilic, with a contact angle of  $0^\circ$  before the ALD process (Figure 5).

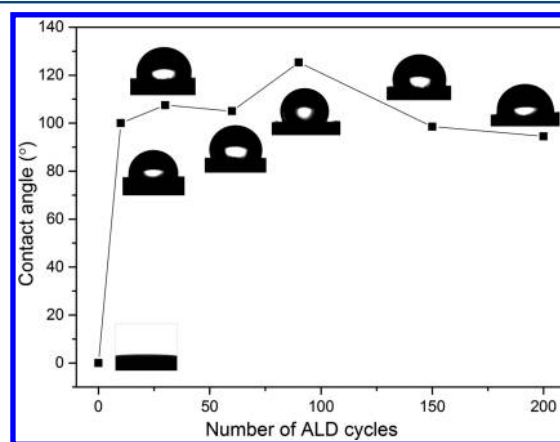


**Figure 5.** Average water contact angles measured on filter papers before and after different ALD  $\text{Al}_2\text{O}_3$  cycles. The insets show the photographs of the water droplet on the filter paper.

Therefore, it is necessary to modify the surface property of the filter paper to enhance its selectivity. The filter paper surface can be modified either to reduce or to increase its hydrophilicity by using appropriate methods. We chose to reduce the hydrophilicity of the filter paper, expecting filter paper with much stronger affinity to oil to allow the penetration of oil yet retain water. The contact angle results showed that the ALD followed by silanization has led to a major enhancement of hydrophobicity (Figure 5). The filter paper subjected to 90 cycles of  $\text{Al}_2\text{O}_3$  ALD followed by silanization with KH-570 displays the highest contact angle to water of

125.3°, which evidently confirms the significantly enhanced hydrophobicity, as water would be easily wetted and spread on the surface of the pristine filter paper. As the ALD deposition cycles further grow up to 150 and 200, the contact angles slightly decrease compared to the 90 cycles of ALD modified filter paper. This might be attributed to the lower surface roughness of the filter paper after 200 ALD cycles, as it can be identified from Figure 4c that some local areas of the filter paper have been merged. Considering that surface roughness plays an important role in wetting, it can be inferred that filter papers with 90 ALD cycles should be more hydrophobic than that with 200 cycles.<sup>27</sup> Wettability measurements showed filter paper with 150 and 200 ALD cycles with contact angles slightly lower than that of 90 cycles, which is consistent with previous report.<sup>28</sup>

As demonstrated in Figure 7c, an oil droplet is absorbed promptly and spread away on the surface; yet the water droplet remains unwetted and stays on the surface for more than 1 h. Interestingly, the areas on the modified filter paper which directly contact the water droplets remained dry, and no marks were left after the water droplet was wiped off gently. These observations suggested the strong hydrophobicity of the modified filter paper. As shown in Figure 7d, with constant addition of water and diesel oil droplets on the modified filter paper covering the opening of the vial underneath, the diesel oil wets and penetrates through the filter paper and drops into the vial. In the meantime, water droplets merge with each other and grow gradually in size on the surface of modified filter paper. With the gravity of the water droplet itself, it does not penetrate the filter paper and yet stays on the surface for a long period of time. It can be concluded that such modified filter papers exhibit selectivity strong enough to effectively separate water and oil.

**3.5. Influence of ALD deposition on the permeation performances of the modified filter papers.** To maintain the high porosity of the pristine filter paper, ALD cycle numbers should be controlled as low as possible to obtain an ultrathin deposition layer on the surface of the filter papers. A continuous deposition layer will be generated covering all the pore walls of the filter paper with the minimum thickness at certain ALD deposition numbers. The filter paper with ALD cycles less than 90 times, i.e., 30, could gradually be wetted by water droplets, indicating insufficiently enhanced hydrophobicity even though the water contact angle increased significantly, as can be seen from Figure 5. In contrast, water droplets on the modified filter paper with a cycle number more than 90 can stay unwetted for a long enough time, implying strong hydrophobicity is achieved. Therefore, the appropriate ALD cycle number can be determined to be around 90, and with a cycle number less than this threshold, the modified filter paper is not hydrophobic enough yet to effectively separate oil from its mixture with water.

We then investigate the permeation of the surface modified filter papers under different conditions. Due to the relatively large pore size of the filter papers (20–25  $\mu\text{m}$ ), permeation can be obtained by the gravity of the liquid itself and no extra pressure was required. As can be seen from Figure 6, the pristine filter paper before surface modification demonstrates a very high water flux of  $1450 \text{ L}\cdot\text{m}^{-2}\cdot\text{h}^{-1}$ , which significantly decreased to around  $250 \text{ L}\cdot\text{m}^{-2}\cdot\text{h}^{-1}$  after  $\text{Al}_2\text{O}_3$  deposition for 10 cycles followed by silanization. With further increase of the ALD cycle numbers up to 200, the flux remained almost unchanged. It is worth mentioning that the water flux

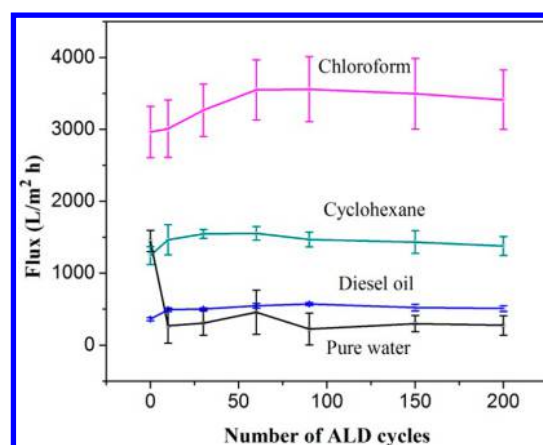


**Figure 6.** Flux of pure water, cyclohexane, diesel oil, and chloroform for filter papers as a function of different ALD cycle numbers.

minimized at 90 ALD cycles; this result confirms that for contact angle, which suggests that 90 ALD cycles of  $\text{Al}_2\text{O}_3$  with the strongest hydrophobicity could be considered as the optimized number. The remarkable change of water flux should be attributed to the transition of the hydrophobicity of the modified filter papers. One may argue that the reduction of effective pore sizes resulting from the formation of an  $\text{Al}_2\text{O}_3$  layer may also account for the reduction of the water flux. However, the thickness of the  $\text{Al}_2\text{O}_3$  layer obtained with cycle number less than 200 is very thin, and its influence on water flux should be negligible, as evidenced by the fact that water flux barely changes when the cycle number increases from 30 to 200. Such a trend in water flux as a function of the ALD cycles indicates the enhancement of the hydrophobicity maximizes at the cycle number of 90. This result is in good consistency with the threshold value of ALD cycle numbers as determined above.

On the contrary, the modified filter paper shows enhanced permeation to various oils, including diesel oil, cyclohexane, and chloroform, compared to the pristine one. Similarly, the oil flux initially increases with rising ALD cycle numbers and then stabilizes, and the peak value occurs around the cycle number of 60 or 90. The flux of various oils for modified filter papers is mainly determined by the density and viscosity of the oils. Chloroform illustrates much larger flux than other oils because of its highest density (1.484 g/mL) and moderate viscosity (0.563 mP·s) whereas diesel oil shows the smallest flux, arising from its highest viscosity (1.5 mP·s) and low density (0.84 g/mL). As for cyclohexane, the viscosity (0.888 mP·s) is in between diesel oil and chloroform; however, the driving force for organic solvents to penetrate the filter paper is gravity. Among the organic solvents, cyclohexane has the lowest density (0.774 g/mL), which implies the weakest driving force to pass through the filter papers. Therefore, it is reasonable that the change of flux for cyclohexane and diesel oil is not as obvious as that for chloroform. The stabilized flux of diesel oil and chloroform for the modified filter paper increased by 39.2% and 15.2%, respectively, compared to the pristine filter paper. Apparently, the improved permeation of oils is also assigned from the enhanced affinity of the modified filter paper toward oils. Considering that the variation in water flux maximizes at the cycle number of 90 and oil flux enhances at 90 as well, we deduce that the optimized modification condition for the filter papers is ALD deposition for 90 cycles followed by silanization.

**3.6. Oil/water separation performances of the modified filter papers.** As discussed above, the pristine filter papers exhibit slightly different affinity to water and oil, and this leads us to investigate the possibility of separating oil and water for unmodified filter papers. The pristine filter paper was placed on top of a vial (Figure 7a), and with the addition of water and

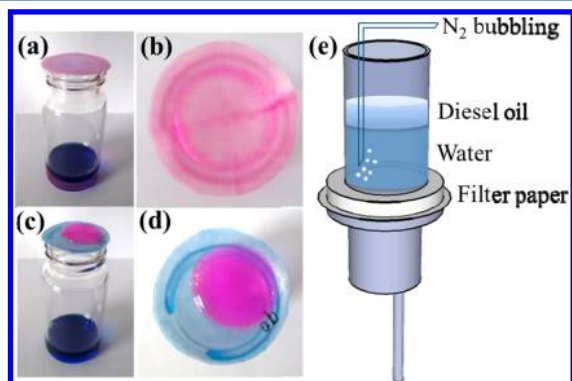


**Figure 7.** Photographs showing the separation and wetting behavior of a diesel oil (blue)/water (red) mixture using pristine filter paper (a: overall, b: top view), modified filter paper (c: overall, d: top view), and the diagram of the filtration cell (e) showing the experimental setup of the separation process for the mixture of water and diesel oil. The sample used in Figure 8c and d was the modified filter paper with 90 ALD cycles followed by KH-570 coupling.

diesel oil, both penetrated through the pristine filter paper and were collected in the vial (Figure 7a). Meanwhile, water droplets spread rapidly on the surface of the filter paper as indicated by the red color of the used filter paper (Figure 7b), which further confirms the previous results that the pristine filter papers cannot be directly used to separate oil/water mixtures.

We then tested the separation efficiency of the modified filter paper, which derived from the ratio between the water left in the filtration cell and the initial feeding water in the separation of different oil/water mixtures.<sup>29</sup> As shown in Figure 8, the overall separation efficiency of the modified filter paper toward all investigated oil/water mixtures is higher than 90% regardless of the density, viscosity, or mass ratio of water and oil, ranging from 1 to 10. Such high separation efficiencies are comparable to other separation systems prepared through complex

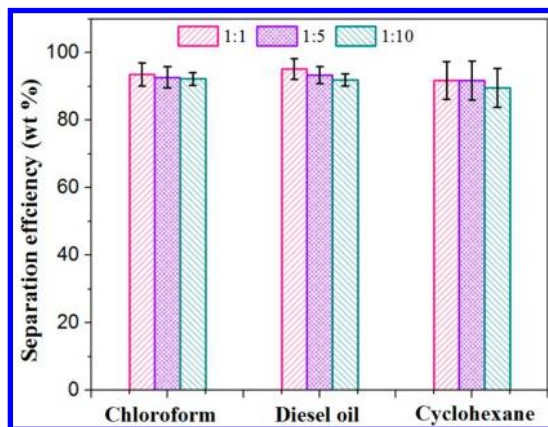


**Figure 8.** Separation efficiencies of the modified filter papers for different oil/water mixture systems (oil:water mass ratio = 1:1, 1:5, 1:10).

modification protocols onto relatively expensive substrates.<sup>30–32</sup> For instance, oleophilic conic copper-based needles were reported with separation efficiencies of around 90%.<sup>33</sup> Research on honeycomb-patterned films by utilizing a specialized coating instrument, which possessed less than 100  $\mu\text{m}$  thickness and superhydrophobicity, was also reported.<sup>34</sup> The methodology we utilized here includes only two steps, the deposition of an oxide layer and silanization, and they consume very limited amounts of materials because both the oxide layer and the silanization layer are extremely thin. The separation efficiencies obtained here are remarkable, especially considering the simple modification methods of low-cost and easily available filter papers.

## 4. CONCLUSIONS

A low-cost paper-based membrane for highly efficient oil/water separation via hydrophobic modification on filter paper is proposed in this work. The modification process is very simple and contains only two steps: a thin alumina layer is first coated by atomic layer deposition onto the surface of filter paper, followed by silane molecules coupled on the precoated alumina layer. The surface modification transforms the filter papers from hydrophilic to hydrophobic and oleophilic, and they exhibit strongly reduced permeation to water and improved permeation to oils. The peculiar wettability is used to separate various types of oil/water mixtures with overall efficiencies greater than 90%. This paper-based membrane is distinguished for its cost-efficient substrates and the simple modification route. This modification method is expected to be easily applied to convert the surface properties of a variety of other substrates from hydrophilic into hydrophobic.

## AUTHOR INFORMATION

### Corresponding Author

\*E-mail: yongwang@njtech.edu.cn. Phone: +86-25-8317 2247. Fax: +86-25-8317 2292.

### Notes

The authors declare no competing financial interest.

## ACKNOWLEDGMENTS

This work is financially supported by the National Natural Science Foundation of China (21176120), the Natural Science Research Program of the Jiangsu Higher Education Institutions (13KJA430005), the Jiangsu Natural Science Funds for Distinguished Young Scholars (BK2012039), and the Project of Priority Academic Program Development of Jiangsu Higher Education Institutions (PAPD).

## REFERENCES

- (1) Nordvik, A. B.; Simmons, J. L.; Bitting, K. R.; Lewis, A.; Strøm-Kristiansen, T. Oil and water separation in marine oil spill clean-up operations. *Spill Sci. Technol. Bull.* **1996**, *3* (3), 107–122.
- (2) Adebajo, M. O.; Frost, R. L.; Klopogge, J. T.; Carmody, O.; Kokot, S. Porous Materials for Oil Spill Cleanup: A Review of Synthesis and Absorbing Properties. *J. Porous Mater.* **2003**, *10* (3), 159–170.
- (3) Chan, Y. J.; Chong, M. F.; Law, C. L.; Hassell, D. G. A review on anaerobic–aerobic treatment of industrial and municipal wastewater. *Chem. Eng. J.* **2009**, *155* (1–2), 1–18.
- (4) Xue, Z.; Cao, Y.; Liu, N.; Feng, L.; Jiang, L. Special wettable materials for oil/water separation. *J. Mater. Chem. A* **2014**, *2* (8), 2445–2460.

- (5) Niu, Z.; Chen, J.; Hng, H. H.; Ma, J.; Chen, X. A Leavening Strategy to Prepare Reduced Graphene Oxide Foams. *Adv. Mater.* **2012**, *24* (30), 4144–4150.
- (6) Sun, H.; Xu, Z.; Gao, C. Multifunctional, Ultra-Flyweight, Synergistically Assembled Carbon Aerogels. *Adv. Mater.* **2013**, *25* (18), 2554–2560.
- (7) Wang, Q.; Wang, X.; Wang, Z.; Huang, J.; Wang, Y. PVDF membranes with simultaneously enhanced permeability and selectivity by breaking the tradeoff effect via atomic layer deposition of TiO<sub>2</sub>. *J. Membr. Sci.* **2013**, *442* (0), 57–64.
- (8) Wang, C.; Yao, T.; Wu, J.; Ma, C.; Fan, Z.; Wang, Z.; Cheng, Y.; Lin, Q.; Yang, B. Facile Approach in Fabricating Superhydrophobic and Superoleophilic Surface for Water and Oil Mixture Separation. *ACS Appl. Mater. Interfaces* **2009**, *1* (11), 2613–2617.
- (9) Feng, L.; Zhang, Z.; Mai, Z.; Ma, Y.; Liu, B.; Jiang, L.; Zhu, D. A Super-Hydrophobic and Super-Oleophilic Coating Mesh Film for the Separation of Oil and Water. *Angew. Chem., Int. Ed.* **2004**, *43* (15), 2012–2014.
- (10) Li, M.; Xu, J.; Lu, Q. Creating superhydrophobic surfaces with flowery structures on nickel substrates through a wet-chemical-process. *J. Mater. Chem.* **2007**, *17* (45), 4772–4776.
- (11) Xue, C.-H.; Jia, S.-T.; Zhang, J.; Tian, L.-Q.; Chen, H.-Z.; Wang, M. Preparation of superhydrophobic surfaces on cotton textiles. *Sci. Technol. Adv. Mater.* **2008**, *9* (3), 035008.
- (12) Matsumoto, H.; Wakamatsu, Y.; Minagawa, M.; Tanioka, A. Preparation of ion-exchange fiber fabrics by electrospray deposition. *J. Colloid Interface Sci.* **2006**, *293* (1), 143–150.
- (13) Cheng, L.-P.; Lin, D.-J.; Yang, K.-C. Formation of mica-intercalated-Nylon 6 nanocomposite membranes by phase inversion method. *J. Membr. Sci.* **2000**, *172* (1–2), 157–166.
- (14) Wang, S.; Li, M.; Lu, Q. Filter Paper with Selective Absorption and Separation of Liquids that Differ in Surface Tension. *ACS Appl. Mater. Interfaces* **2010**, *2* (3), 677–683.
- (15) Nguyen, D. D.; Tai, N.-H.; Lee, S.-B.; Kuo, W.-S. Superhydrophobic and superoleophilic properties of graphene-based sponges fabricated using a facile dip coating method. *Energy Environ. Sci.* **2012**, *5* (7), 7908–7912.
- (16) Zhang, J.; Guo, Z.; Zhi, X.; Tang, H. Surface modification of ultrafine precipitated silica with 3-methacryloxypropyltrimethoxysilane in carbonization process. *Colloids Surf., A* **2013**, *418* (0), 174–179.
- (17) Marichy, C.; Bechelany, M.; Pinna, N. Atomic Layer Deposition of Nanostructured Materials for Energy and Environmental Applications. *Adv. Mater.* **2012**, *24* (8), 1017–1032.
- (18) George, S. M. Atomic Layer Deposition: An Overview. *Chem. Rev.* **2009**, *110* (1), 111–131.
- (19) Detavernier, C.; Dendooven, J.; Pulinthanathu Sree, S.; Ludwig, K. F.; Martens, J. A. Tailoring nanoporous materials by atomic layer deposition. *Chem. Soc. Rev.* **2011**, *40* (11), 5242–5253.
- (20) Wilson, C. A.; Grubbs, R. K.; George, S. M. Nucleation and Growth during Al<sub>2</sub>O<sub>3</sub> Atomic Layer Deposition on Polymers. *Chem. Mater.* **2005**, *17* (23), 5625–5634.
- (21) Spagnola, J. C.; Gong, B.; Arvidson, S. A.; Jur, J. S.; Khan, S. A.; Parsons, G. N. Surface and sub-surface reactions during low temperature aluminium oxide atomic layer deposition on fiber-forming polymers. *J. Mater. Chem.* **2010**, *20* (20), 4213–4222.
- (22) Hyde, G. K.; Scarel, G.; Spagnola, J. C.; Peng, Q.; Lee, K.; Gong, B.; Roberts, K. G.; Roth, K. M.; Hanson, C. A.; Devine, C. K.; Stewart, S. M.; Hojo, D.; Na, J.-S.; Jur, J. S.; Parsons, G. N. Atomic Layer Deposition and Abrupt Wetting Transitions on Nonwoven Polypropylene and Woven Cotton Fabrics. *Langmuir* **2009**, *26* (4), 2550–2558.
- (23) Shi, J.-J.; Ma, W.-S.; Lin, X.-D. Synthesis and Characterization of Functionalized Graphene with KH-570. *Chin. J. Inorg. Chem.* **2012**, *28* (1), 131–136.
- (24) Zhao, H.; Tu, H. Factors that affect the structural and filtration properties of filter papers. *Paper Papermaking* **2006**, *25* (6), 1.
- (25) Hyde, G. K.; Park, K. J.; Stewart, S. M.; Hinstroza, J. P.; Parsons, G. N. Atomic Layer Deposition of Conformal Inorganic Nanoscale Coatings on Three-Dimensional Natural Fiber Systems: Effect of Surface Topology on Film Growth Characteristics. *Langmuir* **2007**, *23* (19), 9844–9849.
- (26) Marin, E.; Lanzutti, A.; Guzman, L.; Fedrizzi, L. Chemical and electrochemical characterization of TiO<sub>2</sub>/Al<sub>2</sub>O<sub>3</sub> atomic layer depositions on AZ-31 magnesium alloy. *J. Coat. Technol. Res.* **2012**, *9* (3), 347–355.
- (27) Jiang, L.; Wang, R.; Yang, B.; Li, T. J.; Tryk, D. A.; Fujishima, A.; Hashimoto, K.; Zhu, D. B. Binary cooperative complementary nanoscale interfacial materials. *Pure Appl. Chem.* **2000**, *72* (1–2), 73.
- (28) Jiang, L.; Zhao, Y.; Zhai, J. A Lotus-Leaf-like Superhydrophobic Surface: A Porous Microsphere/Nanofiber Composite Film Prepared by Electrohydrodynamics. *Angew. Chem., Int. Ed.* **2004**, *43* (33), 4338–4341.
- (29) Pan, Q.; Wang, M.; Wang, H. Separating small amount of water and hydrophobic solvents by novel superhydrophobic copper meshes. *Appl. Surf. Sci.* **2008**, *254* (18), 6002–6006.
- (30) Tu, C.-W.; Tsai, C.-H.; Wang, C.-F.; Kuo, S.-W.; Chang, F.-C. Fabrication of Superhydrophobic and Superoleophilic Polystyrene Surfaces by a Facile One-Step Method. *Macromol. Rapid Commun.* **2007**, *28* (23), 2262–2266.
- (31) Shirtcliffe, N. J.; McHale, G.; I. Newton, M. The superhydrophobicity of polymer surfaces: Recent developments. *J. Polym. Sci., Polym. Phys.* **2011**, *49* (17), 1203–1217.
- (32) Yuan, J.; Liu, X.; Akbulut, O.; Hu, J.; Suib, S. L.; Kong, J.; Stellacci, F. Superwetting nanowire membranes for selective absorption. *Nat. Nano.* **2008**, *3* (6), 332–336.
- (33) Li, K.; Ju, J.; Xue, Z.; Ma, J.; Feng, L.; Gao, S.; Jiang, L. Structured cone arrays for continuous and effective collection of micron-sized oil droplets from water. *Nat. Commun.* **2013**, *4*.
- (34) Yabu, H.; Shimomura, M. Single-Step Fabrication of Transparent Superhydrophobic Porous Polymer Films. *Chem. Mater.* **2005**, *17* (21), 5231–5234.